Engineering xxx (xxxx) xxx

Contents lists available at ScienceDirect

Engineering

journal homepage: www.elsevier.com/locate/eng

Research
Civil Engineering—Review

The Durability of Alkali-Activated Materials in Comparison with Ordinary Portland Cements and Concretes: A Review

Aiguo Wang [a,c], Yi Zheng [a], Zuhua Zhang [b,*], Kaiwei Liu [a], Yan Li [a], Liang Shi [c], Daosheng Sun [a,*]

[a] Anhui Key Laboratory of Advanced Building Materials, Anhui Jianzhu University, Hefei 230022, China
[b] Key Laboratory for Green and Advanced Civil Engineering Materials and Application Technology of Hunan Province, College of Civil Engineering, Hunan University, Changsha 410082, China
[c] Jiangsu Subote New Materials Ltd. Co., Nanjing 211103, China

ARTICLE INFO

Article history:
Received 9 June 2019
Revised 25 July 2019
Accepted 12 August 2019
Available online xxxx

Keywords:
Alkali-activated materials
Geopolymer
Durability
Ordinary Portland cement
Deterioration mechanism

ABSTRACT

China is the largest producer and user of ordinary Portland cement (OPC), and the rapid growth of infrastructure development demands more sustainable building materials for concrete structures. Alkali-activated materials (AAMs) are a new type of energy-saving and environmentally friendly building material with a wide range of potential applications. This paper compares the durability of AAMs and OPC-based materials under sulfate attack, acid corrosion, carbonation, and chloride penetration. Different AAMs have shown distinct durability properties due to different compositions being formed when different raw materials are used. According to the calcium (Ca) concentration of the raw materials, this paper interprets the deterioration mechanisms of three categories of AAMs: calcium-free, low-calcium, and calcium-rich. Conflicts found in the most recent research are highlighted, as they raise concerns regarding the consistence and long-term properties of AAMs. Nevertheless, AAMs show better durability performances than OPC-based materials in general.

1. Introduction

China is the largest producer and user of ordinary Portland cement (OPC). In 2018, the production of 2.4×10^9 t of cement was estimated to consume 3.0×10^9 t of limestone, 7.2×10^8 t of clay, and 3.2×10^9 J of energy, while emitting 2.4×10^9 t of carbon dioxide (CO_2). The CO_2-emission reduction target [1] has driven the entire cement and concrete industry to look for cleaner production technology and alternative binding materials in the past ten years. Alkali-activated materials (AAMs), also known as geopolymers, are manufactured by chemical reactions between an alkaline activator and reactive aluminosilicate materials [2–4]. The reaction process, polymerization mechanism, and products of AAMs have been extensively studied [5–19]. This manufacturing process, which occurs at room temperature or at a slightly elevated temperature (60–80 °C) is completely different from the traditional milling and calcination processes of OPC. Because the raw materials are widely available and include industrial wastes such as slag (SG), steel slag, fly ash (FA), and thermally activated clay (e.g., metakaolin (MK)), AAMs are much more environmentally friendly than OPC. Despite being greener, AAMs have been reported to have mechanical properties that are comparable to those of OPCs and, in most cases, to have superior durability [20].

Depending on the raw materials, different types of AAMs have very different reaction mechanisms, product composition characteristics, and mechanical properties. Zhang [21], Adamiec et al. [22], Lothenbach et al. [23], and Khatib [24] have classified AAMs into calcium-free, low-calcium, and calcium-rich, according to the calcium content in the aluminosilicate raw materials. Representative raw materials are MK, FA, and SG (Fig. 1). Attempts are being made to use many other aluminosilicate raw materials and industrial waste solids to produce AAMs, such as red mud, steel slag, and heated coal gangue. The products of calcium-free/low-calcium systems are mainly zeolite-like (such as analcite, sodalite, etc.) gels, while those of calcium-rich systems are calcium aluminium silicate hydrates (C-(A)-S-H) gels with a low calcium/silicon (Ca/Si) ratio. Attempts have been made to use many other industrial wastes containing potential reactive components to manufacture AAMs; however, trace amounts of components

* Corresponding authors.
E-mail addresses: ZuhuaZhang@hnu.edu.cn (Z. Zhang), sundaosheng@163.com (D. Sun).

https://doi.org/10.1016/j.eng.2019.08.019

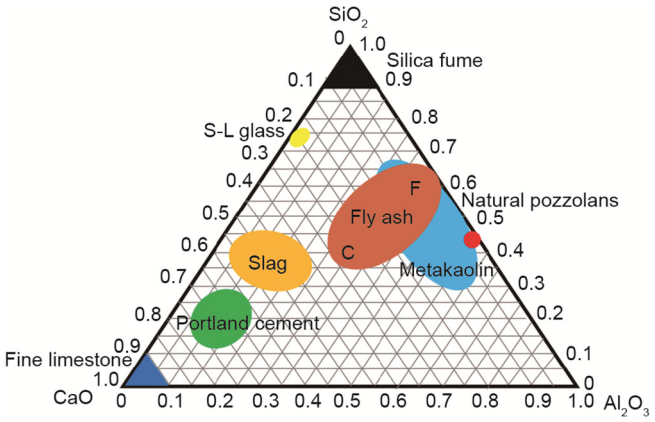

Fig. 1. SiO_2-Al_2O_3-CaO ternary diagram of the aluminosilicate materials MK, FA, and SG, which can be used in AAMs. A comparison of these materials with cement and lime stone is shown. Reproduced from Ref. [22] with permission of Chinese Society of Particuology and Institute of Process Engineering, Chinese Academy of Sciences, © 2008.

present in the industrial wastes may affect the performance of AAMs, especially in terms of durability [25–27].

This review reports on recent studies on the durability of AAMs, particularly in comparison with OPC, for a better understanding of when and where AAMs can be used as OPC alternatives. Four aspects of AAMs durability are summarized: sulfate attack, acid corrosion, carbonation, and chloride penetration. This review provides critical information for further studies toward the development and applications of different AAMs under various conditions.

2. Sulfate attack

Sulfate attack is one of the most serious issues affecting the durability of concrete. The deterioration mechanism includes a set of complex physical and chemical reactions. External or internal sulfate ions of the concrete react with the hydration products of OPC, leading to expansion, cracking and, finally, disintegration of concrete elements [28–32]. C_3A and C_3S contents and concrete density are considered to be the main inter-factors affecting the sulfate resistance of concrete. C_3A is considered to be a key factor in the formation of ettringite, as its hydration product supports the aluminum (Al) phase as a reactant. In addition, the ettringite phase is affected by the content of C_3S, since its hydration product CH is one of the factors contributing to the formation of expandable gypsum and ettringite (Fig. 2) [33,34]. It has also been found that sulfate attack results in decalcification of calcium silicate hydrate (C-S-H) gel, mainly due to the continuous formation of gypsum under low pH conditions as CH is continuously consumed. Thaumasite usually forms when C-S-H gels react, and causes softening of concrete, reduction of strength, and even complete damage [35,36].

Calcium-free AAMs (e.g., MK-based AAM) contain totally different products from OPC systems [37]. Sulfate attack on calcium-free/low-calcium AAMs is an exchange process, in which cations exchange with the components of gels, resulting in increased porosity [38]. However, calcium-rich AAMs (e.g., alkali-activated slag (AAS)) contain C-(A)-S-H gel with a lower Ca/Si ratio than that of C-S-H in an OPC system [39]. The sulfate resistance mechanism of calcium-rich AAM is similar to that of OPC because of the similarity of the reaction (hydration) products. On the other hand, MK-based AAM has a different sulfate resistance mechanism because the main products are sodium aluminosilicate hydrate (N-A-S-H) gel. Therefore, the design and use of AAMs as sulfate-resistant alternatives to OPC should involve a careful consideration of the type of AAM.

Karakoç et al. [39] found that the compressive strength of AAS decreased with the increase of $MgSO_4$ concentration and immersion time, while the appearance showed little change after 24 weeks of immersion. Alcamand et al. [38] adjusted the content of CaO and the matrix composition (in terms of the SiO_2/Al_2O_3 molar ratio) of AAM by adding slag and silica fume into MK-based AAM. Ideally, this AAM structure should be stable enough to resist sulfate attack. However, the Ca^{2+} in (C, N)-A-S-H gel can be exchanged by external cations during sulfate attack. Therefore, the incorporation of Ca has a certain negative effect on sulfate resistance. It is evident from this research that N-A-S-H gel, as the main product in low-calcium/calcium-free AAMs, has a better resistance to sulfate attack (Fig. 3). In comparison, C-(A)-S-H gel, as the main product in calcium-rich AAM, has worse sulfate resistance to the formation of gypsum and ettringite [38,40,41].

In many previous studies on the durability of AAMs, it was highlighted that AAMs produced from MK do not produce sulfate-aluminate minerals such as ettringite during the hydration process. Ettringite- and gypsum-type sulfate attack products are avoided, so calcium-free or low-calcium AAMs have better resistance to sulfate attack [37,42–48]. Tao et al. [49] investigated the sulfate resistance

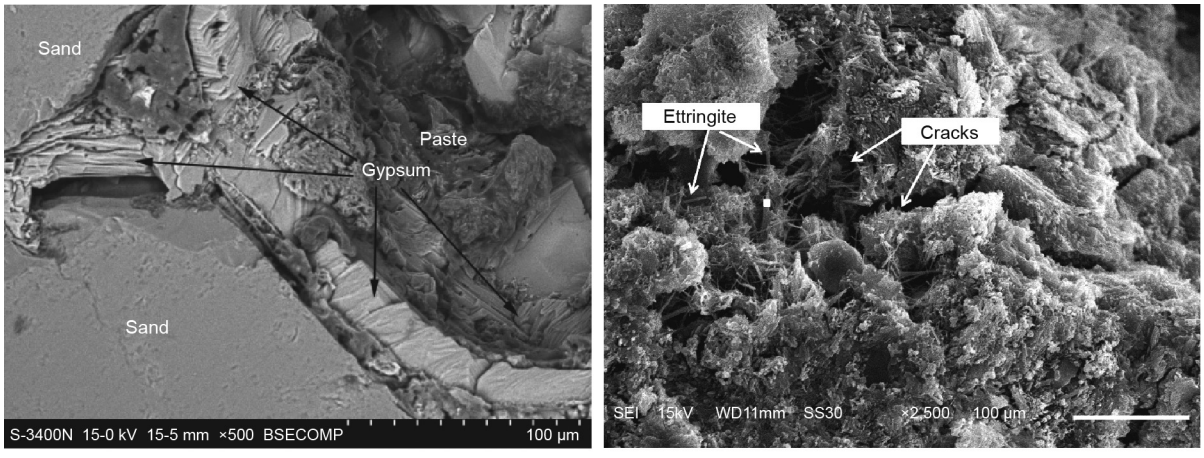

(a) (b)

Fig. 2. Microstructure of OPC mortars after sulfate attack in Na_2SO_4 solution. (a) Gypsum formation; (b) ettringite formation. Reproduced from Ref. [34] with permission of co-author KW Liu, @2010.

Please cite this article as: A. Wang, Y. Zheng, Z. Zhang et al., The Durability of Alkali-Activated Materials in Comparison with Ordinary Portland Cements and Concretes: A Review, Engineering, https://doi.org/10.1016/j.eng.2019.08.019

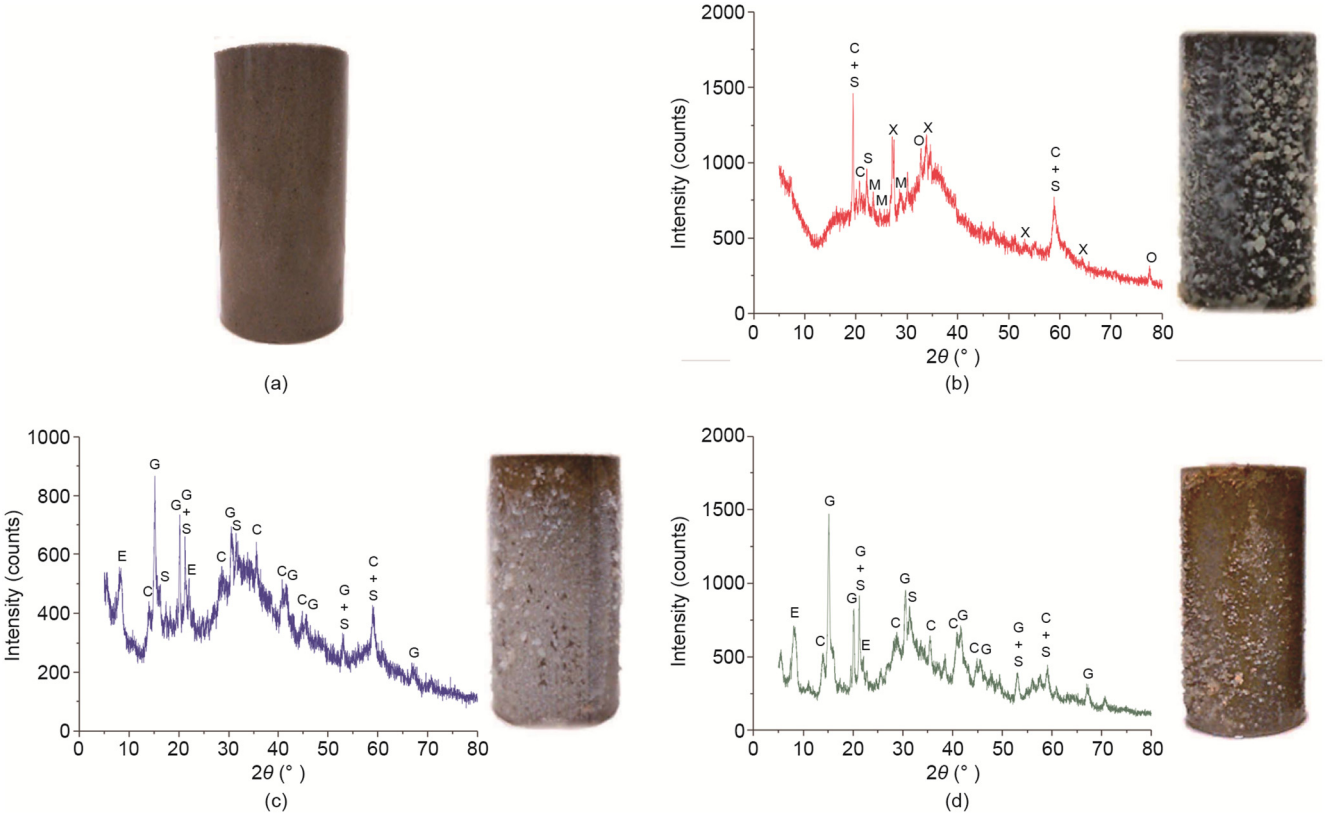

Fig. 3. Minerals formed on the surface of the specimens after 180 d of magnesium sulfate attack. (a) Sound AAM made with 100% MK; (b) 80/20 MK/silica fume; (c) 80/20 MK/SG; (d) 60/40 MK/SG. M: magnesium sulfate, C: sodium carbonate, X: sodium silicate, S: sodium sulfate, O: silicon oxide, E: etringite; G: gypsum. Reproduced from Ref [38] with permission of Elsevier Ltd. and Techna Group S.r.l., ©2018.

by measuring the strength retention rate; their results showed that the strength retention rate of MK-based AAM was much higher than that of OPC in Na_2SO_4 solution after 28 d. Hou et al. [50] found significant differences in the compressive strength and apparent density of FA-based AAM after 150 d of immersion in different sulfate solutions, and considered that the effect of the sulfate solution on the properties of FA-based AAM was related to diffusion. In addition, the durability of the samples in sulfate solution was related to the type of cation of the activator, the cation in the sulfate solution, and the concentration of the solution.

Tang et al. [51] found that during sulfate attack, both the compressive strength of FA-based AAM concrete and that of OPC concrete showed a decreasing trend first, followed by an increasing trend. The mass change of the attacked group was not large (as shown in Fig. 4) in 5% Na_2SO_4 solution. FA-based AAM concrete prepared with recycled aggregate showed high compressive strength rather than damage in 5% Na_2SO_4 solution with a dry-wet cycle [52]. Palomo et al. [53] and Bakharev [54] had similar conclusions. In a study of the performance change and microstructure evolution of FA-based AAM in a sulfate environment, Tang et al. [55] found that there were no crack or spalling phenomena after sulfate attack for 60 d. It was concluded that FA-based AAMs will not produce expansive products that are harmful to the structure in a sodium sulfate environment.

Džunuzović et al. [56] studied the effect of Na_2SO_4 solution on the durability of alkali-activated FA–SG blended materials (Table 1). The composition change of the Na_2SO_4 solution was analyzed. The Si found in the solution may be from the dissolution of the unreacted alkaline activator component of the AAM or the silicon-rich component of the gel structure. The increase of Ca concentration in the solution indicates that the calcium-containing hydrates such as C-S-H gel and C-(A)-S-H gel have poor sulfate attack resistance compared with the N-A-S-H gel. Ismail et al. [57] suggested that dissolution of Ca in AAM may be due to the reaction with Na_2SO_4 or ion exchange in sulfate solution. Zheng et al. [58] studied the sodium sulfate resistance of AAM mortars and cement mortar under dry-wet cycling conditions. It was found that the coefficient of compressive strength of AAM mortars was better than that of OPC mortars after 75 cycles. AAM mortars contained only the sodium sulfate phase as corrosion products.

Elyamany et al. [59] found that the water absorption and porosity of FA-based AAM decreased with the increase of curing temperature and molar concentration of the activator, and that the corrosion resistance to $MgSO_4$ was therefore improved. However, gypsum crystals were detectable in the AAM samples after $MgSO_4$ corrosion, and the microcracks after corrosion were attributed to the formation of gypsum. Jin et al. [60] found that the compressive strength of FA-based AAM first decreased and then increased in 5% $MgSO_4$ solution, which indicated that the diffusion of Mg^{2+} into AAM concrete and the migration of alkali metal cations into the solution occur simultaneously. It can be inferred that the two processes will eventually reach equilibrium after a long period of two-way ion diffusion. This evidence shows that the Ca concentration of AAMs and the sulfate type (i.e., sodium or magnesium) are the two most critical factors affecting their sulfate resistance performance.

Sulfate attack is a dynamic process for both OPC and AAM, and the corrosion mechanisms depend on the nature of the hydration products. The attack on OPC mainly consists of a series of chemical reactions and physical impacts that generate extra crystals and internal stress. Normally, the softening of cement concrete is due to the decalcification of C-S-H gel, while expansion and cracking of the structure are caused by the formation of gypsum and

Please cite this article as: A. Wang, Y. Zheng, Z. Zhang et al., The Durability of Alkali-Activated Materials in Comparison with Ordinary Portland Cements and Concretes: A Review, Engineering, https://doi.org/10.1016/j.eng.2019.08.019

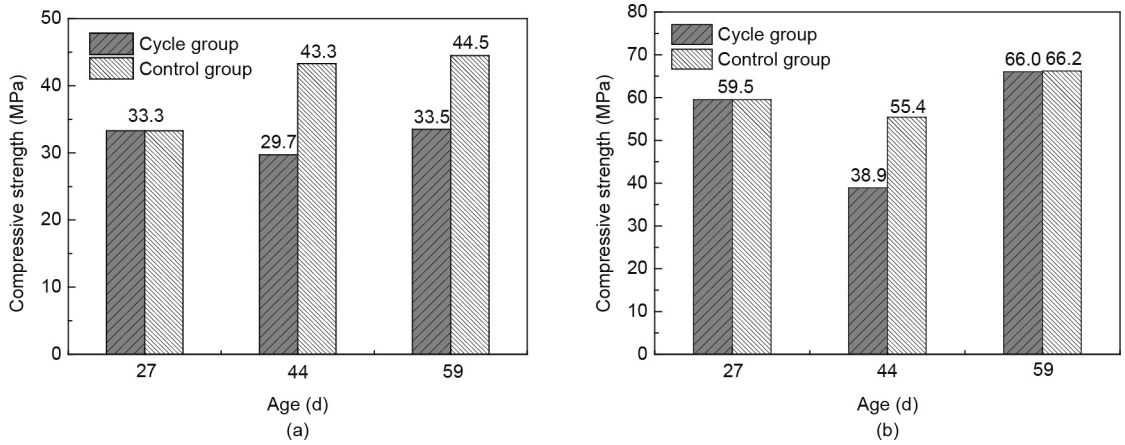

Fig. 4. Compressive strength of (a) OPC concretes and (b) FA-based AAM concretes after immersion in 5% Na_2SO_4 solutions for 27–59 d. Reproduced from Ref. [51] with permission of Material Reports, © 2015.

Table 1
pH and composition analysis of the 5% Na_2SO_4 solution before and after interaction with alkali-activated FA-SG materials.

Time (d)	pH	Ion concentration in Na_2SO_4 solution ($mg \cdot L^{-1}$)				
		Na	Si	Ca	Al	Mg
0	6.04	14 140	6	5.4	0.7	0.9
30	13.11	14 760	143	31.4	2.4	0.9
90	11.30	17 880	52	73.6	0.5	0.9
180	11.25	16 880	32	71.2	0.8	0.9

ettringite [61]. Calcium-rich AAMs usually produce C-(A)-S-H gel, so the sulfate attack mechanism is more or less similar to that of OPC. For calcium-free or low-calcium AAMs, however, the ion exchange reaction occurs between the sulfate solution and the network-like structure. During the attack, the pores of the network structure of the N-A-S-H gel change, and microcracks are gradually formed, leading to deterioration of the AAM structure.

3. Acid corrosion

The acid corrosion resistance of OPC cements and concretes is rather poor because of the nature of high pH and the porous matrix. Acid can react with CH and C-S-H gel in cement concrete to form non-gelling or water-soluble substances, resulting in the destruction of concrete. Acid corrosion also causes the decomposition of calcium silicate hydrates and calcium aluminates hydrates, and thus destroys the cementitious binder and reduces the strength of the concrete [62]. Wang et al. [63] found that the surface of concrete soaked in acid solution (pH = 2) first formed a layer of white sticky substance, and then became softened. Ning et al. [64] found that acid corrosion began at the surface of the sample, and the extent of corrosion in the concrete was inversely proportional to the pH value of the solution. Alexander et al. [65] reported that CH on the surface of OPC was first consumed by the reaction with acid, which increased the porosity and allowed the acid to erode the interior part. With a drop in the pH of the pore solution below 12.4, C-S-H gel will decalcify, accompanied by the dissolution of Al_2O_3–Fe_2O_3-mono (AFm) and Al_2O_3–Fe_2O_3-tri (AFt).

AAMs usually show better acid resistance than OPC [66–68]. Table 2 summarizes recent research findings on different acids that attack AAMs [68–75]. Decalcification also occurs in calcium-rich AAM; however, because AAMs have lower permeability than OPC, this process is much slower. In addition, a dense layer of aluminosilicate gel can prevent corrosion [76,77].

Bouguermouh et al. [72] considered that the main factors affecting the acid resistance of AAMs were the mineral composition of the aluminosilicate raw materials and the types of alkali metal cation in the activators. The N-A-S-H gel in MK-based AAM was only slightly affected by acid corrosion (0.1 $mol \cdot L^{-1}$ HCl). Although cracks caused by shrinkage of the gel layer did exist, the material still maintained a good structure. Jin et al. [78] found that the appearance of MK-based AAM remained almost unaffected during the corrosion cycle of acid rain (molar ratio SO_4^{2-}/NO_3^{-} = 3/4); X-ray diffraction (XRD) analysis showed no significant compositional change.

Zheng et al. [79] immersed FA-based AAM in 5% H_2SO_4 solution for 28 d, and found that the specimen still met the acid soaking safety index of the Chinese standard GB 50212–2002 "Specification for construction and acceptance of anticorrosive engineering of buildings." Zhao et al. [80] reported that N-A-S-H gel, as the main product of FA-based AAM, has good HCl resistance, and that the structure was slightly affected by acid. When the concentration of calcium in the FA is high or when the acid type changes, the acid resistance may decrease. Mehta and Siddique [81] found that the SO_4^{2-} in sulfuric acid will react with Ca^{2+} in the product to form $CaSO_4$ (as shown in Fig. 5), in addition to H^+ reacting with the body material in the corrosion process of FA-based AAM. The interaction of two corrosion processes aggravates the deterioration of the sample.

Both AAMs and OPC are alkaline materials, and a neutralization process occurs when they come into contact with acid. The findings reported in Table 2 indicate that the acid resistance of AAMs is generally better than that of OPC due to their intrinsic composition and structural characteristics. Shi and Stegemann [82] and Beddoe and Schmidt [83] reported that the corrosion resistance of cement paste depended on the protective layer or on the hydration product itself, rather than on the pore permeability of hardened paste during the process of acid corrosion. Gutberlet et al. [84] studied the resistance of OPC to H_2SO_4 acid corrosion at pHs

Please cite this article as: A. Wang, Y. Zheng, Z. Zhang et al., The Durability of Alkali-Activated Materials in Comparison with Ordinary Portland Cements and Concretes: A Review, Engineering, https://doi.org/10.1016/j.eng.2019.08.019

Table 2
Research works on different types of acid corrosion of AAMs.

AAM (activator)	Experimental conditions	Performance changes	Comments	Ref.
FA	H_2SO_4 12 months	Compressive strength decreases by 65%	Acid reacts directly with sample, causing structural degradation	[69]
FA and SG (NaOH + sodium silicate)	H_2SO_4 (pH = 0.8) 9 months	FA-based: Mass loss is 5.4%. Compressive strength decreases by 10.9% SG-based: Mass loss is 9.6%. Compressive strength decreases by 7.3%	AAMs are more stable than OPC	[70]
FA (NaOH + sodium silicate)	HCl (pH = 1.0) 90 d	Weight loss of 2.5%. Strength decreases by 23%	HCl causes N-A-S-H gel to degrade Al and generate SiO_2-rich zeolite	[71]
MK (NaOH + sodium silicate/ KOH + potassium silicate)	HCl (pH = 1.47) 28 d	Surface of the sample is slightly degraded and the color is unchanged	Secondary minerals in products can alleviate acid corrosion	[72]
MK (KOH + potassium silicate)	HCl (pH = 2.0) 28 d	Geopolymer structure remains after 28 d of corrosion	K^+ and H^+ undergo ion exchange in the product structure	[73]
SG (sodium silicate)	CH_3COOH (pH = 4.5) 150 d	Sample strength retention rate is about 75%	Aluminosilicate gel produced by decalcification is small and mechanical strength is higher	[68]
FA (NaOH/KOH + sodium silicate)	CH_3COOH (pH = 2.4) 6 months	About 40% strength loss	The structure and acid corrosion products of AAM prepared by different activators are different	[74]
SG plus FA (NaOH + sodium silicate)	Organic acid (pH = 3.0) 18 weeks	As the content of Ca decreases, the mass loss of the sample decreases, and the residual compressive strength increases	Corrosion resistance: C-S-H < C-(A)-S-H < N-A-S-H	[75]

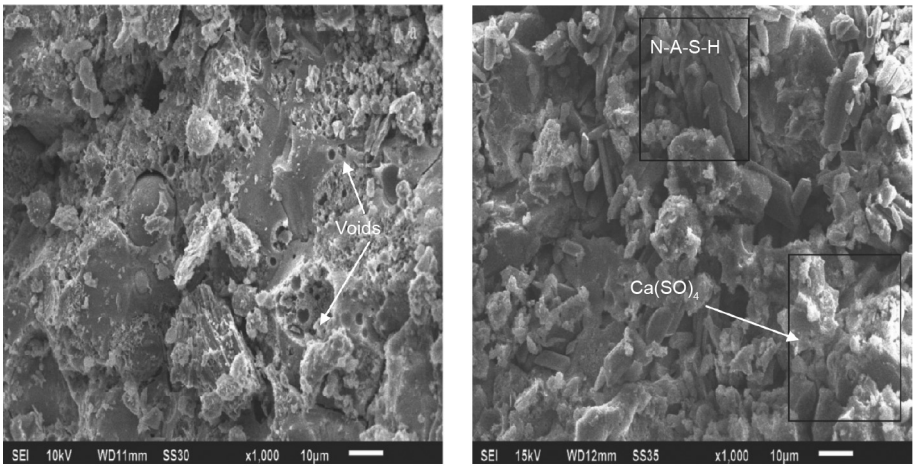

(a) (b)

Fig. 5. Scanning electron microscope (SEM) images of FA-based AAM with the addition of 10% OPC (a) before and (b) after corrosion in 5% H_2SO_4 solution for 365 d. Reproduced from Ref. [81] with permission of Elsevier Ltd., © 2017.

of 2, 3, and 4, respectively, and found that the surface of OPC will form a porous layer. The transition zone between the deteriorated layer and the non-corroded material is shown in Fig. 6. The surface layer and the transition zone are the key factors that determine the durability of materials. If the surface layer is relatively dense, it can effectively isolate and protect the internal material from further acid corrosion.

4. Carbonation

The carbonation of concrete refers to a neutralization process in which the acidic gas CO_2 in the air reacts with the aqueous alkaline substance of the concrete, resulting in a decrease of alkalinity and a change in the chemical composition of the concrete [85]. Carbonation itself produces no obvious damage to OPC concrete. The main problem is the decrease of alkalinity causes damage to passivation film of protects the steel bar. With the participation of water and air, the steel will rust; eventually, the structure will be destroyed due to the internal expansion stress [86]. Shi et al. [87] pointed out that the carbonation reaction can lower the pH value of concrete from an initial value above 13 to roughly 8. It also causes changes in the pore size distribution and the porosity of hardened cement paste. Furthermore, it will affect the diffusion of harmful ions (i.e., Cl^-, SO_4^{2-}) in concrete. The C-S-H gel is preferably present as an irregular cluster structure instead of as a densely arranged structure [88]. The decrease in the pH of the pore solution during carbonation accelerates the decomposition of Friedel salts (calcium monochlorate aluminate) in hardened cement paste, which increases both the porosity and the diffusion coefficient of Cl^- in concrete [89,90]. Papadakis [91] simulated the carbonation process of cement-based materials as follows: First, CO_2 diffuses into the pores of cement-based materials, while the hydration product CH dissolves in the pore solution. Then, CO_2 dissolves in the pore solution and reacts with CH to form $CaCO_3$. Normally, the main products of natural carbonation for CH are calcite, nepheline, and aragonite [92]. The carbonation process is accompanied by microstructural changes, such as the formation of $CaCO_3$,

Please cite this article as: A. Wang, Y. Zheng, Z. Zhang et al., The Durability of Alkali-Activated Materials in Comparison with Ordinary Portland Cements and Concretes: A Review, Engineering, https://doi.org/10.1016/j.eng.2019.08.019

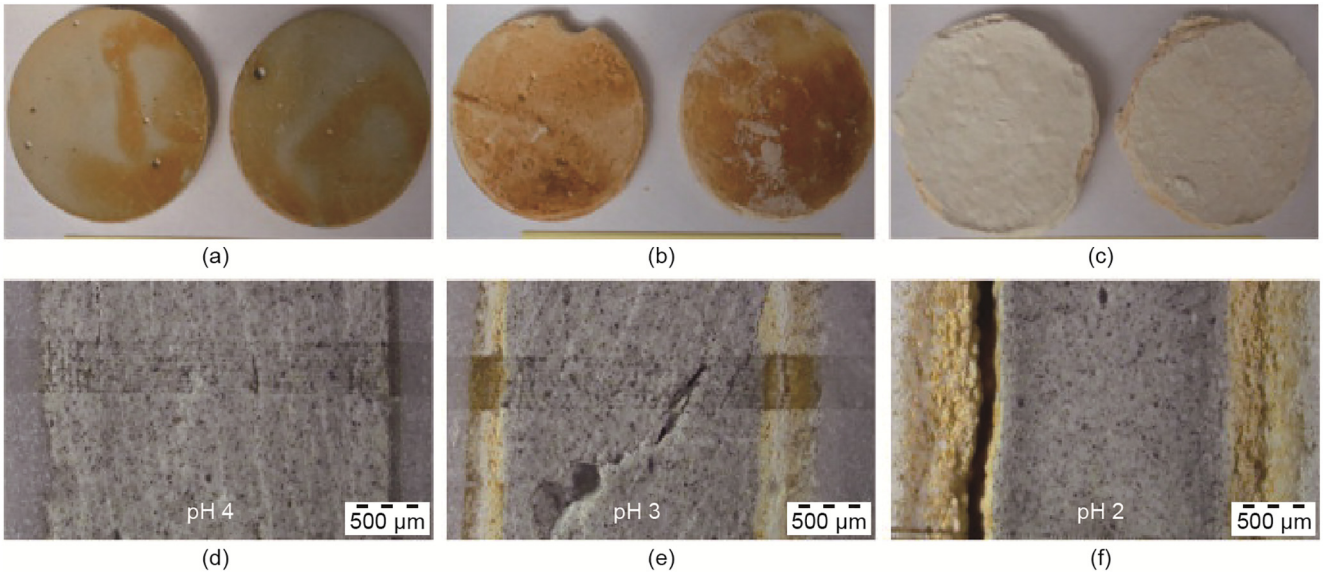

Fig. 6. (a–c) Degraded OPC samples after storage in H_2SO_4 solution for 28 d at a pH of (a) 4, (b) 3, and (c) 2. (d–f) Micrographs of the corresponding cross-sections. Reproduced from Ref. [84] with permission of Elsevier Ltd., © 2015.

polymerization of decalcified C-S-H gel, and decomposition of ettringite [93]. C-S-H gel and CH, as the main cement hydration products, are prone to carbonization [94]. The process of C-S-H gel carbonation involves the decalcification of C-S-H gel and, finally, the formation of amorphous gel. The whole process is accompanied by an overall reduction in the volume of the products and an increase in porosity and pore size [95,96].

The carbonation mechanism of AAMs differs from that of OPC. Moreover, the reaction mechanisms of AAMs in calcium-rich and low-calcium systems are different. During the carbonation process of calcium-rich AAMs, CO_2 dissolves into the pore solution to form carbonic acid, and directly reacts with C-(A)-S-H gel to form $CaCO_3$. However, N-A-S-H gel, the main product in the low-calcium system, does not undergo the decalcification process, and carbonation of N-A-S-H gel in this case is mainly the transformation of the pore solution from high alkalinity to a high concentration of sodium carbonate [97,98].

Products of AAS are mainly C-(A)-S-H gels with low crystallinity and a uniform and dense amorphous feature. In carbonation, since the product does not contain CH, the dynamic equilibrium of Ca^{2+} is directly maintained by the decalcification of C-(A)-S-H gel [99]. Due to decalcification, C-(A)-S-H gel undergoes volume shrinkage and an increased degree of polymerization. Further carbonation transforms the gel into silica gel, resulting in greater shrinkage [100]. In the case of natural carbonation, the main carbonation product of AAS is $Na_2CO_3{\cdot}10H_2O$; under accelerated carbonation conditions, it is $NaHCO_3$ [101]. Chen et al. [102,103] found that the carbonation rate of AAS mortar was higher than that of OPC mortar during accelerated carbonation with 20% CO_2 concentration. Carbonation will cause a large shrinkage of mortar, which will result in microcracks around the aggregate, and will increase the porosity of the paste and the CO_2 diffusion coefficient of the mortar. Yu et al. [104] reported that the amount of activator can affect the carbonation resistance of AAS. With an increase of sodium silicate, the carbonation resistance of AAS can gradually be improved under accelerated carbonation conditions with 20% CO_2 concentration. Dong et al. [105] used mineral powder and Pisha sandstone as raw materials to prepare AAMs and conducted a carbonation study under accelerated conditions. They reported that the carbonation resistance was enhanced when the amount of NaOH was increased.

For low-calcium AAMs, Li ZG and Li S [106] found that the number of microcracks in FA-based AAM decreased significantly after the carbonation process under the conditions of 5% CO_2 concentration, and the microstructure of the FA-based AAM became denser, as shown in Fig. 7. The pH of the pore solution decreased substantially to about 11 throughout the carbonation process. Bernal et al. [107] proposed that the main product of FA-based AAM, N-A-S-H gel, is stable during carbonation. However, the dissolution of N-A-S-H will occur only when OH^- from the pore solution reacts with carbonic acid. When calcium is added—for example, by blending SG in FA-based AAM [106] or blending SG in MK-based AAM [108]—the carbonation resistance of AAMs generally decreases.

According to Pouhet and Cyr [109], the carbonation reaction in the pore solution of calcium-free AAMs with natural CO_2 content can be divided into two separate phases followed by stabilization of the pH: Phase 1 comprises the nearly complete carbonation of the pore solution during the first two weeks of exposure to atmospheric CO_2, resulting in the formation of Na_2CO_3 and a pH value of around 12 being reached. Phase 2 comprises the evolution of the carbonate/bicarbonate phase equilibrium, resulting in the formation of bicarbonate (10% at 180 d) and a pH of around 10.5. The pH value of the pore solution is higher than the steel depassivation limit of 9. The compressive strength of MK-based AAM remains unchanged (Fig. 8).

It can be concluded that the carbonation resistance of AAMs is not as good as that of OPC, but that the pH value of AAMs after carbonation can be maintained at above 10.5. However, there are a few conflicting findings. Huang et al. [110] reported that the strength of OPC improved after a carbonation test with 20% CO_2 concentration, while the strength of FA-based AAM was not affected by carbonation. Sufian Badar et al. [111] prepared FA-based AAM under accelerated carbonation for 450 d, and found a remarkable decrease in the pH, a consequent increase in the total porosity, and a reduction in the mechanical strength properties.

The reported differences in the carbonation resistance of AAMs are probably related to differences in measurement methods. According to Huang et al. [112], phenolphthalein indicator and the pH value cannot effectively determine the carbonation resistance of FA-based AAM. Yu et al. [104] reported that the test method has an impact on the measurement of the carbonation

Please cite this article as: A. Wang, Y. Zheng, Z. Zhang et al., The Durability of Alkali-Activated Materials in Comparison with Ordinary Portland Cements and Concretes: A Review, Engineering, https://doi.org/10.1016/j.eng.2019.08.019

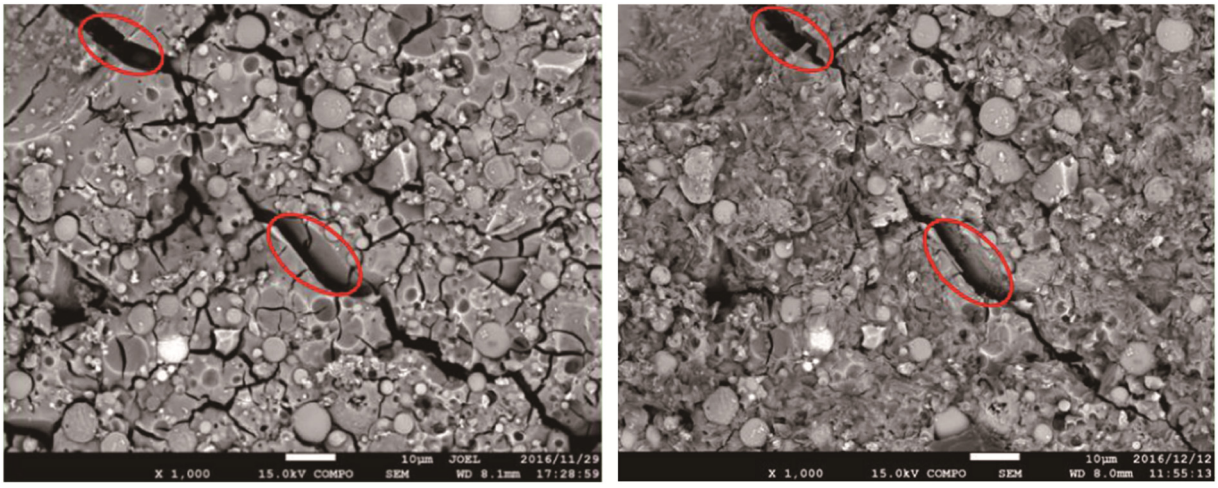

Fig. 7. SEM images of FA-based AAM (a) before and (b) after a carbonation test with 5% CO_2 concentration. Reproduced from Ref. [106] with permission of Elsevier Ltd., © 2018.

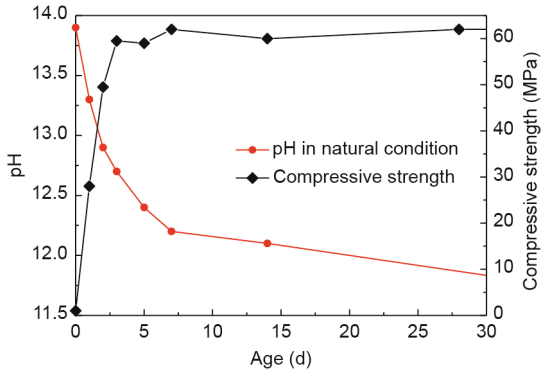

Fig. 8. pH evolution of the pore solution and compressive strength of MK-based AAM cured under natural CO_2 content. Reproduced from Ref. [109] with permission of Elsevier Ltd., © 2016.

resistance of AAMs. The results obtained by the electrochemical method and the borehole sampling method are more consistent than those obtained using phenolphthalein indicator. Natural carbonation and accelerated carbonation will also affect the experimental results. Bernal et al. [101] proved that the carbonation products of AAS by these two methods are different. The increase in CO_2 concentration will directly affect the equilibrium of CO_3^{2-}/HCO_3^-, and will thus have a significant influence on the pH value. When OPC is carbonized, the consequent pH value, mineral composition, and pore structure also depend on CO_2 concentration [113].

In addition, the characteristics of the raw materials used to prepare the AAMs will affect the carbonation results. There is no standard, and just a few recommendations have been made; for example, FA-based AAM needs a high concentration of NaOH solution, and curing at 60 °C for 48 h will result in more complete polymerization [114,115]. The physical and chemical characteristics of the raw materials differ from one place to another, resulting in differences in the properties and microstructure of the AAMs [116]. Bernal et al. [117] considered that AAS microstructure development greatly depends on the chemical compositions and mineral compositions of SG. The type of activators and binder volume of AAS will exert a great influence on the carbonation resistance. Furthermore, the water content of the porous structure in AAS will affect the carbonation experiment. It has been shown that when the relative humidity (RH) of the OPC pore structures varies between 50% and 70%, the CO_2 diffusion rate is promoted, whereas when the RH is higher than 70%, the CO_2 diffusion rate will decrease because pores are filled with water [118]. These differences in the raw materials, experimental conditions, and internal water content will surely lead to different results in the carbonation resistance of AAMs.

Efflorescence is a process that involves carbonation. The efflorescence reaction is similar to the carbonation reaction of calcium-free/low-calcium AAMs (the corrosion process only consumes free alkali and the substrate will not cause damage) [119,120]. Kani et al. [121] pointed out that when the concrete column touched damp soil at the bottom, water migrated to the surface of the concrete through capillary action and evaporated, and soluble alkali dissolved, reacted with CO_2 from the air, and eventually precipitated on the surface of the concrete with water evaporation. Pouhet and Cyr [109] pointed out that efflorescence did not cause real durability problems for OPC, but could affect the appearance.

AAMs contain large amounts of soluble alkali (e.g., NaOH and KOH). Provis et al. [122] reported that Na^+ is not stable in the network structure and can be dissolved in the pore solution of AAMs. Several reasons for efflorescence have been determined, and include: ① Efflorescence can be caused by the open pores of AAMs and a low degree of polymerization; ② an excessive amount of alkali activator leads to high alkali concentration in the pore solution; and ③ Na^+ has a poor binding ability with the network structure of AAMs [123–125].

Zhang et al. [119,126] considered that the main factors influencing the efflorescence of FA-based AAM involve the alkali content of the activator, the type of activator, and the curing temperature. Among these factors, the alkali content of the activator was considered to be the most important factor affecting efflorescence. Free alkali inside the AAM will cause efflorescence under partially dry and wet conditions (as shown in Fig. 9). The larger pores and higher total porosity in the internal structure of the AAM contribute to fast alkali leaching, causing more severe efflorescence. However, efflorescence on the surface of the sample will not change the mineral composition of the material itself.

Please cite this article as: A. Wang, Y. Zheng, Z. Zhang et al., The Durability of Alkali-Activated Materials in Comparison with Ordinary Portland Cements and Concretes: A Review, Engineering, https://doi.org/10.1016/j.eng.2019.08.019

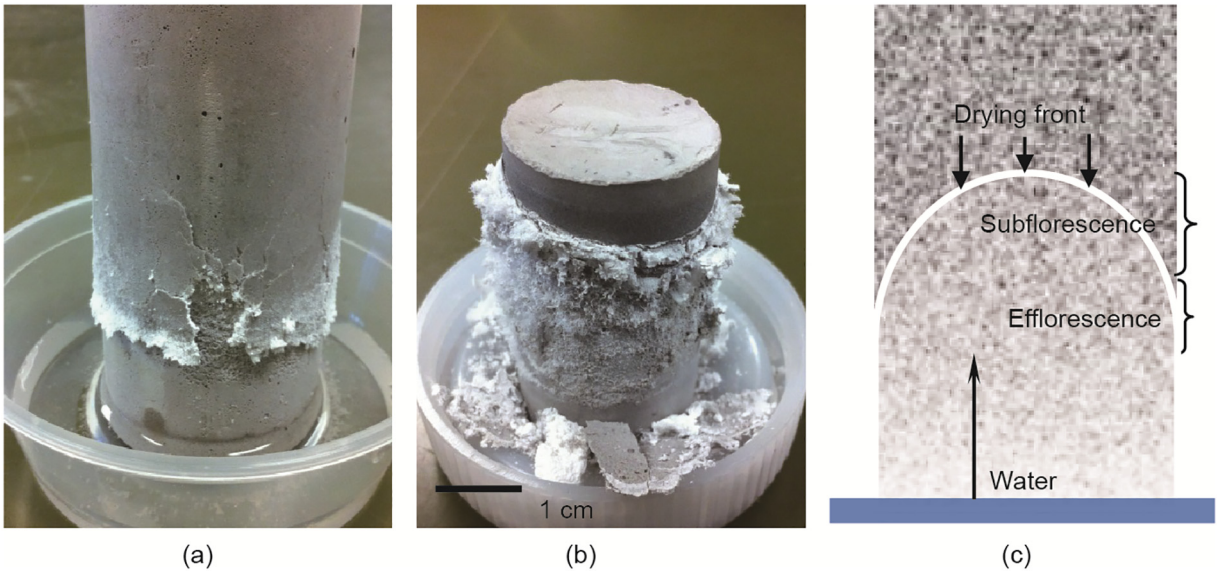

Fig. 9. (a) Deterioration of FA-based AAM after 7 d in contact with water at the bottom; (b) deterioration of low-temperature cured FA-based AAM after 90 d of exposure to simulated efflorescence conditions with the regular addition of water at the bottom; (c) schematic drying of FA-based AAM in contact with water and the consequent crystallization. Reproduced from Ref. [119] with permission of Elsevier Ltd., © 2018.

5. Chloride penetration

Chloride penetration is the major factor that leads to steel corrosion in concrete. Due to its significant effect, chloride penetration is an important issue for concrete durability. Corrosion damage of steel-reinforced OPC concrete structures under the attack of Cl^- usually manifests as surface corrosion of reinforcement bars and the cracking and spalling of concrete cover due to the formation of expansive products during steel corrosion [127]. Cl^- ions in concrete come from two sources: internal Cl^- from the components of concrete mixtures and external Cl^- from the environment. Partial Cl^- dissolves in the pore solution as free chloride, and partial Cl^- is combined in the cement hydration products by means of chemical/physical binding [128]. The main factor affecting chloride ion penetration is the porosity of the cement paste. The coarser the pore structure is, the more open the pores are, and the greater the penetration is. The capability of the cement binder to solidify chloride ions also affects the permeability of chloride ions in concrete [129,130]. Martín-Pérez et al. [127] pointed out that the chloride-binding capacity of cementitious materials has an important effect on the chloride migration rate and steel corrosion in concrete. Xie et al. [130] reported that steel corrosion occurred when free Cl^- reached the surface of the steel bar at a certain concentration. Because carbonation will affect the pore structure of the cement paste, there is a close relationship (a coupling effect) between carbonation and chloride penetration. This is a complex process of Cl^- migration in concrete, which simultaneously includes diffusion, capillary absorption, and infiltration [131]. The factors affecting the chloride resistance of OPC concrete in studies [129–137] are shown in Table 3.

AAMs have a dense microstructure and the chemical compositions of pore solution are complex; however, the relationship between chloride penetration and porosity follows a similar trend as in OPC systems, albeit with a lower penetration rate [138]. For example, the chloride penetration coefficient of FA-based AAM is one third that of OPC at the same strength grade [139]. At present, chloride ion transport test methods for OPC concretes include the natural diffusion method and various accelerated diffusion methods [132]. Further research is required to know whether these methods can be directly applied to perform chloride penetration testing on AAMs.

Researchers [140–148] systematically studied the factors influencing the chloride penetration of AAMs, which are summarized in Table 4 and Fig. 10. Zhou [149] found that when a NaOH solution with a higher concentration was used in the manufacture of AAM, a higher reaction extent of FA was achieved, and the porosity and chloride penetration were subsequently reduced. Calcium-rich AAMs are considered to have better anti-chloride permeability than OPC. With an increase in age, the durability advantage of AAS over OPC is more obvious [150]. Shi et al. [151] showed that the AAS reaction product, C-(A)-S-H gel and the hydrotalcite phase, could adsorb Cl^-, and that there was less free Cl^- in the early stage

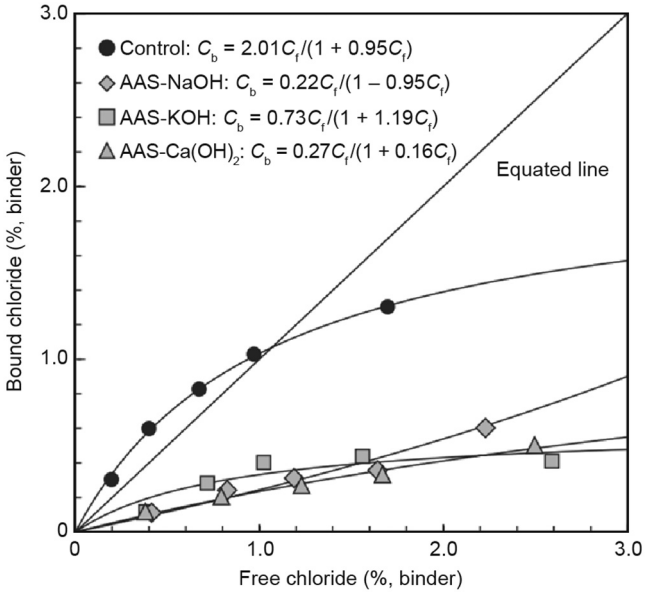

Fig. 10. Langmuir isotherm fittings between free and bound chlorides depending on the activator type of AAS [141]. C_b: concentration of bound chloride; C_f: concentration of free chloride.

Please cite this article as: A. Wang, Y. Zheng, Z. Zhang et al., The Durability of Alkali-Activated Materials in Comparison with Ordinary Portland Cements and Concretes: A Review, Engineering, https://doi.org/10.1016/j.eng.2019.08.019

Table 3
Factors affecting the chloride penetration of OPC concrete.

Factors		Results	Refs.
Internal factors	Adsorption of cementitious materials	OPC itself has a certain adsorption effect on Cl^-	[131]
	Water–cement ratio	The Cl^- diffusion coefficient increases with an increase of the water–cement ratio	[132,133,134]
	C_3A content	There is higher resistance of chloride attack with an increase of C_3A content	[129]
	Pore characteristics	There is worse resistance to chloride penetration with higher pore connectivity and larger pore size	[135]
External factors	Mineral admixture	Mineral admixtures can refine the pore structure of concrete and reduce the chloride penetration rate	[130,133]
	Corrosion time	The apparent diffusion coefficient decreases with the increase of corrosion time	[131,133,134]
	Ambient temperature	The Cl^- permeability rate increases with the increase of temperature	[131,136,137]
	Stress	In the state of compressive stress, the diffusion coefficient is smaller than in the unstressed state; in the tensile stress state, the diffusion coefficient is larger than in the unstressed state	[131]
	Cracking	There is an increased Cl^- diffusion coefficient of concrete in the crack area	[131]

Table 4
Factors affecting the chloride penetration of AAMs.

Influencing factor	Results	Refs.
Type of activators	The penetration of chloride in AAM activated by sodium silicate powder is much higher than that of water glass	[140]
	The penetration of chloride in KOH- and NaOH-activated AAM is similar to that in OPC. When CH is used as an activator, the corrosion resistance is improved (Fig. 10)	[141]
Type of raw materials	AAS has better anti-chloride penetration than FA-based AAM under the same conditions	[142]
Content of raw materials	The chloride penetration of AAMs decreases with the increase of raw materials	[140]
Content of alkali	Very complex; no obvious trend	[140,143,144]
Modulus of water glass	An appropriate modulus of water glass can increase the density of AAMs, which is beneficial to reduce the penetration of chloride	[145]
		[146]
Content of water	Low water content of the matrix will help improve anti-chloride penetration; this trend is in agreement with OPC systems	[147,148]

of chloride penetration, so the reinforcement had no obvious rust phenomenon in this period.

Chen et al. [152] discovered that the penetration of Cl^- in hardened AAS paste mainly depended on connected pores. The utilization of silica fume in the AAS improved the resistance to chloride penetration, since silica fume effectively filled the pores and refined the pore structure. Zhang et al. [153] added lithium SG into AAS and obtained reduced chloride permeability, mainly because of the adsorption of Cl^- onto the structure and the filling effect of lithium SG particles. In addition, Khan et al. [154] found that due to the formation of the hydrotalcite-like phase, AAS binders have a better capacity for Cl^- adsorption than OPC. It was reported that the two types of layered double hydroxides (LDHs)—that is, the magnesium–aluminum (Mg-Al) hydrotalcite-like phase and strätlingite—that are present as the two reaction products in AAS both have Cl^- uptake capacity, but their mechanisms are different: Chloride uptake in hydrotalcite structures is governed by surface adsorption, while that in strätlingite shows the formation of a hydrocalumite-like phase and ion exchange [155].

6. Conclusions and perspectives

This paper presents the most recent research results from durability studies on AAM materials and OPC systems in terms of sulfate attack, acid corrosion, carbonization, and chloride penetration. The following conclusions can be drawn based on the results and discussion:

(1) In general, AAMs have better durability than OPC. However, calcium-free/low-calcium AAMs and calcium-rich AAMs show significant differences in specific durability studies due to the difference in reaction products. The mechanisms of strength loss, pore structure change, cracking due to chemical attacks on N-A-S-H in calcium-free AAMs, and cracking due to chemical attacks on C-(A)-S-H in calcium-rich AAMs are substantially different. Furthermore, because of the similarity of the products of calcium-rich AAMs (e.g., AAS) and OPC, the degradation mechanisms of binders and their concretes that are exposed to carbonation, acid, and sulfate attack are more or less the same.

(2) The raw materials used to manufacture AAMs are no longer only MK, FA, and SG. Attempts are being made to use a wide range of solid wastes. At present, the core aim of using solid wastes is to recycle. Thus far, not much effort has been spent on relevant standards to guide this utilization. Some minor components (e.g., MgO) in raw materials may have unknown effects on the durability of AAMs. This raises concern in industry, and deserves more research in the future.

(3) Durability tests of AAMs are based on the testing methods for OPC cements and concretes. AAMs and OPC-based materials differ in terms of reaction mechanism, products, and microstructures, and it is still controversial whether such testing methods are applicable or reasonably reflect the true trend of durability. This topic requires further validation in both laboratory and field study (which will only be practicable when a certain volume of AAMs is used in the future).

(4) Some upgrading technologies can improve the corrosion resistance of AAMs, mainly by achieving a higher degree of reaction, refined pore structure, and an improvement of density. The utilization of an appropriate amount of nano-SiO_2 in AAMs can improve the microstructure of the products and the carbonation resistance. LDHs have interlayer ion exchangeability, which can uptake chloride ions and other harmful ions that penetrate into cementitious materials. The incorporation of LDHs into AAMs holds great potential for enhancing their durability.

Acknowledgements

Financial support from the National Natural Science Foundation of China (51778003, 51878263, and 51608004), Opening Foundation of State Key Laboratory of High Performance Civil Engineering Materials (2018CEM002), Anhui Provincial Education Department (gxfxZD2016134), and Anhui Province Higher Education Revitalization Program ([2014]No.11).

Please cite this article as: A. Wang, Y. Zheng, Z. Zhang et al., The Durability of Alkali-Activated Materials in Comparison with Ordinary Portland Cements and Concretes: A Review, Engineering, https://doi.org/10.1016/j.eng.2019.08.019

Compliance with ethics guidelines

Aiguo Wang, Yi Zheng, Zuhua Zhang, Kaiwei Liu, Yan Li, Liang Shi, and Daosheng Sun declare that they have no conflict of interest or financial conflicts to disclose.

References

[1] Gao TM, Shen L, Shen M, Liu LT, Chen FN, Gao L. Evolution and projection of CO_2 emissions for China's cement industry from 1980 to 2020. Renew Sust Energ Rev 2017;74:522–37.
[2] Davidovits J. Geopolymers of the first generation: siliface-process. Geopolymer 1988;1:49–67.
[3] Davidovits J. Geopolymers and geopolymeric materials. Therm Anal Calorim 1989;35(2):429–41.
[4] Palomo A, Grutzeck MW, Blanco MT. Alkali-activated fly ashes: a cement for the future. Cement Concr Res 1999;29(8):1323–9.
[5] Van Deventer JSJ, Provis JL, Duxson P. Technical and commercial progress in the adoption of geopolymer cement. Miner Eng 2012;29:89–104.
[6] Mehta A, Siddique R. An overview of geopolymers derived from industrial by-products. Constr Build Mater 2016;127:183–98.
[7] Singh B, Ishwarya G, Gupta M, Bhattacharyya SK. Geopolymer concrete: a review of some recent developments. Constr Build Mater 2015;85:78–90.
[8] Provis JL, Palomo A, Shi CJ. Advances in understanding alkali-activated materials. Cement Concr Res 2015;78:110–25.
[9] Roy DM. Alkali-activated cements opportunities and challenges. Cement Concr Res 1999;29(2):249–54.
[10] Agrawal US, Wanjari SP, Naresh DN. Characteristic study of geopolymer fly ash sand as a replacement to natural river sand. Constr Build Mater 2017;150:681–8.
[11] Provis JL, Van Deventer JSJ. Geopolymerisation kinetics. 1. *In situ* energy-dispersive X-ray diffractometry. Chem Eng Sci 2007;62(9):2309–17.
[12] Nikolov K, Rostovsky I, Nugteren H. Geopolymer materials based on natural zeolite. Case Stud Constr Mater 2017;6:198–205.
[13] Komnitsas K, Zaharaki D. Geopolymerisation: a review and prospects for the minerals industry. Miner Eng 2007;20(14):1261–77.
[14] Zhang ZH, Zhu HJ, Zhou CH, Wang H. Geopolymer from kaolin in China: an overview. Appl Clay Sci 2016;119:31–41.
[15] Luukkonen T, Abdollahnejad Z, Yliniemi J, Kinnunen P, Illikainen M. One-part alkali-activated materials: a review. Cement Concr Res 2018;103:21–34.
[16] Papa E, Medri V, Amari S, Manaud J, Benito P, Vaccari A, et al. Zeolite-geopolymer composite materials: production and characterization. J Clean Prod 2018;171:76–84.
[17] Belmokhtar N, Ammari M, Brigui J, Allal LB. Comparison of the microstructure and the compressive strength of two geopolymers derived from metakaolin and an industrial sludge. Constr Build Mater 2017;146:621–9.
[18] Provis JL. Alkali-activated materials. Cement Concr Res 2018;114:40–8.
[19] Fan F, Liu Z, Xu G, Peng H, Cai C. Mechanical and thermal properties of fly ash based geopolymers. Constr Build Mater 2018;160:66–81.
[20] Zhang YJ, Yang MY, Kang L, Zhang L, Zhang K. Research progresses of new type alkali-activated cementitious material catalyst. J Inorg Mater 2016;31(3):225–33. Chinese.
[21] Zhang ZH. Performance and reaction mechanism of a metakaolin based inorganic geopolymer [dissertation]. Nanjing: Nanjing University of Technology; 2010. Chinese.
[22] Adamiec P, Benezet JC, Benhassaine A. Pozzolanic reactivity of silico-aluminous fly ash. Particuology 2008;6(2):93–8.
[23] Lothenbach B, Scrivener K, Hooton RD. Supplementary cementitious materials. Cement Concr Res 2011;41(12):1244–56.
[24] Khatib JM. Sustainability of construction materials. London: Woodhead Publishing Limited and CRC Press; 2009.
[25] Wang X, Yan BL, Liu C, Jiang LZ, Liu T. Complex calcium and silicate-aluminates industry wastes combined active phosphorous slag. J B Univ Technol 2009;35(9):112–20. Chinese.
[26] Chen M, Sun ZP, Liu JS. State of the art review on activating techniques and mechanism of phosphorus slag. Mater Rev 2013;27(21):112–6. Chinese.
[27] Peng XQ, Liu C, Li S, Jiang Y, Zeng L. Research on the setting and hardening performance of alkali-activated steel slag-slag based cementitious materials. J Hunan Univ 2015;42(6):47–52.
[28] Feng P, Miao C, Bullard JW. A model of phase stability, microstructure and properties during leaching of Portland cement binders. Cem Concr Compos 2014;49(12):9–19.
[29] Jin YN, Zhou SX. Types and mechanism of concrete sulfate attack. J East China Jiaotong Univ 2006;23(5):4–8. Chinese.
[30] Fang XW, Shen CN, Yang DB, Chen ZH. Zhang ZF. Investigations of influence factor on the rate of concrete sulfate attack. J Build Mater 2007;10(1):89–96. Chinese.
[31] Ouyang CS, Nanni A, Chang WF. Internal and external sources of sulfate ions in portland cement mortar: two types of chemical attack. Cement Concr Res 1988;18(5):699–709.
[32] Chen JK, Jiang MT, Zhu J. Damage evolution in cement mortar due to corrosion of sulphate. Corros Sci 2008;50(9):2478–83.
[33] Liu K, Deng M, Mo L. Influence of pH on the formation of gypsum in cement materials during sulfate attack. Adv Cement Res 2015;27(8):487–93.
[34] Liu KW. Process and mechanism of deterioration of cementitious materials soaked in sodium sulfate solutions [dissertation]. Nanjing: Nanjing University of Technology; 2010. Chinese.
[35] Chen JK, Qian C, Song H. A new chemo-mechanical model of damage in concrete under sulfate attack. Constr Build Mater 2016;115:536–43.
[36] Shen XD, Li ZJ. Cement and concrete for marine applications. Beijing: Chemical Industry Press; 2016. Chinese.
[37] Yuan L, Shi HS, Wang ZL. Research and development status of geopolymeric cement. Hou Mater App 2002;30(2):21–4. Chinese.
[38] Alcamand HA, Borges PHR, Silva FA, Trindade ACC. The effect of matrix composition and calcium content on the sulfate durability of metakaolin and metakaolin/slag alkali-activated mortars. Ceram Int 2018;44(5):5037–44.
[39] Karakoç MB, Türkmen I, Maraş MM, Kantarci F, Demirboğa R. Sulfate resistance of ferrochrome slag based geopolymer concrete. Ceram Int 2016;42(1):1254–60.
[40] Yan X, Jiang L, Guo M, Chen Y, Song Z, Bian R. Evaluation of sulfate resistance of slag contained concrete under steam curing. Constr Build Mater 2019;195:231–7.
[41] Thokchom S, Ghosh P, Ghosh S. Performance of fly ash based geopolymer mortars in sulphate solution. J Eng Sci Tech Rev 2010;3(1):36–8.
[42] Duan P, Yan C, Zhou W. Influence of partial replacement of fly ash by metakaolin on mechanical properties and microstructure of fly ash geopolymer paste exposed to sulfate attack. Ceram Int 2016;42(2):3504–17.
[43] Ren D, Yan C, Duan P, Zhang Z, Li L, Yan Z. Durability performances of wollastonite, tremolite and basalt fiber-reinforced metakaolin geopolymer composites under sulfate and chloride attack. Constr Build Mater 2017;134:56–66.
[44] Sata V, Sathonsaowaphak A, Chindaprasirt P. Resistance of lignite bottom ash geopolymer mortar to sulfate and sulfuric acid attack. Cem Concr Compos 2012;34(5):700–8.
[45] Chindaprasirt P, Paisitsrisawat P, Rattanasak U. Strength and resistance to sulfate and sulfuric acid of ground fluidized bed combustion fly ash–silica fume alkali-activated composite. Adv Constr Build Mater Powder Technol 2014;25(3):1087–93.
[46] Liu J, Shi D, Zhang WS, Ye JY, Zhang JB. Study on the mechanism of alkali-activated cementitious materials prepared with calcium silicate slag. Bull Chin Ceram Soc 2014;33(1):6–20. Chinese.
[47] Zhang J, Shi CJ, Zhang ZH, Ou ZH. Durability of alkali-activated materials in aggressive environments: a review on recent studies. Constr Build Mater 2017;152:598–613.
[48] Lu J, Kang CY, Li Q. Properties and microstructure of sodium silicate activated cementitious materials. Bull Chin Ceram Soc 2017;36(10):3412–6. Chinese.
[49] Tao WH, Fu XH, Sun FJ, Yang ZX. Studies on properties and mechanisms of geopolymer cementitious material. Bull Chin Ceram Soc 2008;27(4):730–5. Chinese.
[50] Hou YF, Wang DM, Zhou WJ, Lu HB, Wang L. Study on sulfate-resistance of fly ash-based geopolymers. New Build Mater 2008;35(7):41–4. Chinese.
[51] Tang L, Huang Q, Wang QY, Zhang HE, Shi XS. Research on corrosion resistance and relevant mechanism of geopolymer concrete and ordinary concrete in the same sulfate solution. Mater Rev 2015;29(6):129–34. Chinese.
[52] Tang L, Zhang HE, Huang Q, Wang QY, Shi XS. Research on resistance to sulfates of fly ash based geopolymeric recycled concrete. J Sichuan Univ 2015;47(S1):164–70. Chinese.
[53] Palomo A, Blanco-Varela MT, Granizo ML, Puertas F, Vazquez T, Grutzeck MW. Chemical stability of cementitious materials based on metakaolin. Cement Concr Res 1999;29(7):997–1004.
[54] Bakharev T. Durability of geopolymer materials in sodium and magnesium sulfate solutions. Cement Concr Res 2005;35(6):1233–46.
[55] Tang L, Wang QY, Zhang HE, Huang Q, Shi XS. Performance and microstructure of fly ash base geopolymer concrete in sulfate solution. Concrete 2016;1:112–5. Chinese.
[56] Džunuzović N, Komljenović M, Nikolić V, Ivanović T. External sulfate attack on alkali-activated fly ash-blast furnace slag composite. Constr Build Mater 2017;157:737–47.
[57] Ismail I, Bernal SA, Provis JL, Hamdan S, Van Deventer JSJ. Microstructural changes in alkali activated fly ash/slag geopolymers with sulfate exposure. Mater Struct 2013;46(3):361–73.
[58] Zheng JR, Yang CL, Chen YZ. Discussion on the mechanism of the resistance of alkali-activated cementing material to external sulfate attack. J Zhengzhou Univ 2012;33(3):4–7. Chinese.
[59] Elyamany HE, Abd Elmoaty AEM, Elshaboury AM. Magnesium sulfate resistance of geopolymer mortar. Constr Build Mater 2018;184:111–27.
[60] Jin MT, Chen Y, Dong HL. Research on sulfate attack resistance of the geopolymer solidification MSWI fly ash. J Zhejiang Univ Technol 2013;41(6):596–600. Chinese.
[61] El-Hachem R, Rozière E, Grondin F, Loukili A. Multi-criteria analysis of the mechanism of degradation of Portland cement based mortars exposed to external sulphate attack. Cement Concr Res 2012;42(10):1327–35.
[62] Tang XY, Xiao J, Chen F. Effect and research progress of acid deposition on concrete durability. Mater Rev 2006;20(10):97–101. Chinese.
[63] Wang K, Ma BG, Long SZ, Luo ZT. Acid rain attack on different variety of cement concretes. J Wuhan Univ Technol 2009;31(2):1–4. Chinese.
[64] Ning BK, Chen SL, Zhang Q, Piao YZ, Hu DW. Double corrosion effects under acid and freezing and thawing corrosion and fracture behavior of concrete. J Shenyang Univ Technol 2005;27(5):575–8. Chinese.

Please cite this article as: A. Wang, Y. Zheng, Z. Zhang et al., The Durability of Alkali-Activated Materials in Comparison with Ordinary Portland Cements and Concretes: A Review, Engineering, https://doi.org/10.1016/j.eng.2019.08.019

[65] Alexander M, Bertron A, Belie ND. Performance of cement-based materials in aggressive aqueous environments. Berlin: Springer; 2013.
[66] Rüscher CH, Mielcarek E, Lutz W, Ritzmann A, Kriven WM. Weakening of alkali-activated metakaolin during aging investigated by the molybdate method and infrared absorption spectroscopy. J Am Ceram Soc 2010;93(9):2585–90.
[67] Jirasit F, Rüscher CH, Lohaus L, Chindaprasirt P. Durability performance of alkali-activated metakaolin, slag, fly ash, and hybrids. In: Developments in strategic ceramic materials II: Ceramic engineering and science proceedings. Hoboken: Wiley Press; 2017. p. 1–12.
[68] Bernal SA, Rodriguez ED, De Gutierrez RM, Provis JL. Performance of alkali-activated slag mortars exposed to acids. J Adv Cem Based Mater 2012;1(3):138–51.
[69] Sumajouw DMJ, Wallah SE, Hardjito D. On the development of fly ash-based geopolymer concrete. ACI Mater J 2004;101(6):467–72.
[70] Albitar M, Ali MSM, Visintin P, Drechsler M. Durability evaluation of geopolymer and conventional concretes. Constr Build Mater 2017;136:374–85.
[71] Fernandez-Jimenez A, García-Lodeiro I, Palomo A. Durability of alkali-activated fly ash cementitious materials. J Mater Sci 2007;42(9):3055–65.
[72] Bouguermouh K, Bouzidi N, Mahtout L, Pérez-Villarejo L, Martínez-Cartas ML. Effect of acid attack on microstructure and composition of metakaolin-based geopolymers: the role of alkaline activator. J Non-Cryst Solids 2017;463:128–37.
[73] Gao XX, Michaud P, Joussein E, Rossignol S. Behavior of metakaolin-based potassium geopolymers in acidic solutions. J Non-Cryst Solids 2013;380(12):95–102.
[74] Bakharev T. Resistance of geopolymer materials to acid attack. Cement Concr Res 2005;35(4):658–70.
[75] Koenig A, Herrmann A, Overmann S, Dehn F. Resistance of alkali-activated binders to organic acid attack: assessment of evaluation criteria and damage mechanisms. Constr Build Mater 2017;151:405–13.
[76] Lloyd RR, Provis JL, Van Deventer JSJ. Acid resistance of inorganic polymer binders. 1. Corrosion rate. Mater Struct 2012;45(1–2):1–14.
[77] Zhao JW, Cui C, Ge YP, Xiao B, Peng H, Zhang JR. Recent development of research on durability of geopolymer for civil structural applications. Bull Chin Ceram Soc 2016;35(9):2832–40. Chinese.
[78] Jin MT, Zheng ZD, Sun Y, Chen LW, Jin ZF. Resistance of metakaolin-MSWI fly ash based geopolymer to acid and alkaline environments. J Non-Cryst Solids 2016;450:116–22.
[79] Zheng JR, Liu LN, Xie LX. Properties of the mortar and concrete of alkali-activated fly-ash cementing materials. Concrete 2009;5:77–9. Chinese.
[80] Zhao XH, Liu CY, Zuo LM, Pang YZ, Liu YF. Experimental research on durability of new grouting materials with soda residue and fly ash matrix. Indus Constr 2018;48(3):31–6. Chinese.
[81] Mehta A, Siddique R. Sulfuric acid resistance of fly ash based geopolymer concrete. Constr Build Mater 2017;146:136–43.
[82] Shi CJ, Stegemann JA. Acid corrosion resistance of different cementing materials. Cement Concr Res 2000;30(5):803–8.
[83] Beddoe RE, Schmidt K. Acid attack on concrete—effect of concrete composition: part 1. Cem Int 2009;7:88–94.
[84] Gutberlet T, Hilbig H, Beddoe RE. Acid attack on hydrated cement—effect of mineral acids on the degradation process. Cement Concr Res 2015;74:35–43.
[85] Ashraf W. Carbonation of cement-based materials: challenges and opportunities. Constr Build Mater 2016;120:558–70.
[86] Šavija B, Luković M. Carbonation of cement paste: understanding, challenges, and opportunities. Constr Build Mater 2016;117:285–301.
[87] Shi CJ, Pavel VK, Della R. Alkali-activated cements and concretes. Beijing: Chemical Industry Press; 2008. Chinese.
[88] Hussain S, Bhunia D, Singh SB. Comparative study of accelerated carbonation of plain cement and fly-ash concrete. Build Eng 2016;10:285–301.
[89] Morandeau A, Thiery M, Dangla P. Impact of accelerated carbonation on OPC cement paste blended with fly ash. Cement Concr Res 2015;67:226–36.
[90] Li SB, Sun W. Review on deterioration of concrete subjected to coupling effect of fatigue load, carbonation and chlorides. J Chin Ceram Soc 2013;41(11):1459–64. Chinese.
[91] Papadakis VG. Fundamental modeling and experimental investigation of concrete carbonation. ACI Mater J 1991;88(4):363–73.
[92] Goñi S, Gaztañaga MT, Guerrero A. Role of cement type on carbonation attack. J Mater Res 2002;17(7):1834–42.
[93] Martínez-Ramírez S, Fernández-Carrasco L. Carbonation of ternary cement systems. Constr Build Mater 2012;27(1):313–8.
[94] Ho LS, Nakarai K, Ogawa Y, Sasaki T, Morioka M. Effect of internal water content on carbonation progress in cement-treated sand and effect of carbonation on compressive strength. Cem Concr Compos 2018;85:9–21.
[95] Borges PHR, Costa JO, Milestone NB, Lynsdale CJ, Streatfield RE. Carbonation of CH and C-S-H in composite cement pastes containing high amounts of BFS. Cement Concr Res 2018;109:184–97.
[96] Shah V, Scrivener K, Bhattacharjee B, Bishnoi S. Changes in microstructure characteristics of cement paste on carbonation. Cement Concr Res 2018;109:184–97.
[97] Ye HL, Radlińska A. Carbonation-induced volume change in alkali-activated slag. Constr Build Mater 2017;144:635–44.
[98] Criado M, Palomo A, Fernández-Jiménez A. Alkali activation of fly ashes. Part 1: effect of curing conditions on the carbonation of the reaction products. Fuel 2005;84(16):2048–54.
[99] He J, He JH, Wang YB. Carbonation characteristics of alkali-activated slag cementitious materials. Bull Chin Ceram Soc 2015;34(4):927–30. Chinese.
[100] McGinnis PB, Shelby JE. Diffusion of water in float glass melts. J Non-Cryst Solids 1994;177:381–8.
[101] Bernal SA, Provis JL, Brice DG, Kilcullen A, Duxson P, van Deventer JSJ. Accelerated carbonation testing of alkali-activated binders significantly underestimates service life: the role of pore solution chemistry. Cement Concr Res 2012;42(10):1317–26.
[102] Chen XX, Gao HL, Weng LQ, Chen W. Research on carbonation process of alkali-activated cement mortars. J Wuhan Univ Technol 2014;36(3):18–22. Chinese.
[103] Chen XX, Gao HL, Weng LQ, Chen W, Li GX. Research on the performance of alkali-activated cement mortars mixed with seawater. J Wuhan Univ Technol 2014;36(12):1–5. Chinese.
[104] Yu X, Yu X, Jiang X, Zhang JY, Hua Q, Yuan JN. Study on reinforced alkali-activated slag mortar carbonation resistance and rebar corrosion. Concrete 2015;11:110–3. Chinese.
[105] Dong JL, Zhang TT, Wang LJ. Alkali-activated modified steel slag/Pisha sandstone composites. Acta Mater Com Sin 2016;33(1):132–41. Chinese.
[106] Li ZG, Li S. Carbonation resistance of fly ash and blast furnace slag based geopolymer concrete. Constr Build Mater 2018;163:668–80.
[107] Bernal SA, Provis JL, Walkley B, Nicolas RS, Gehman JD, Brice DG, et al. Gel nanostructure in alkali-activated binders based on slag and fly ash, and effects of accelerated carbonation. Cement Concr Res 2013;53(2):127–44.
[108] Bernal SA, Provis JL, Gutiérrez RMD, Van Deventer JSJ. Accelerated carbonation testing of alkali-activated slag/metakaolin blended concretes: effect of exposure conditions. Mater Struct 2015;48(3):653–69.
[109] Pouhet R, Cyr M. Carbonation in the pore solution of metakaolin-based geopolymer. Cement Concr Res 2016;88:227–35.
[110] Huang Q, Shi XS, Wang QY, Tang L. Research on carbonation of fly ash geopolymeric concrete. Chin Rura Water Hydr 2015;7:121–5. Chinese.
[111] Sufian Badar M, Kupwade-Patil K, Bernal SA, Provis JL, Allouche EN. Corrosion of steel bars induced by accelerated carbonation in low and high calcium fly ash geopolymer concretes. Constr Build Mater 2014;61:79–89.
[112] Huang Q, Shi XS, Wang QY, Tang L, Zhang HE. Effect of recycled coarse aggregate on carbonation resistance of fly ash geopolymeric concrete. Bull Chin Ceram Soc 2015;34(5):1264–9. Chinese.
[113] Anstice DJ, Page CL, Page MM. The pore solution phase of carbonated cement pastes. Cement Concr Res 2005;35(2):377–83.
[114] Monteiro PJ. Scaling and saturation laws for the expansion of concrete exposed to sulfate attack. Proc Natl Acad Sci USA 2006;103(31):11467–72.
[115] Hadi MNS, Al-Azzawi M, Yu T. Effects of fly ash characteristics and alkaline activator components on compressive strength of fly ash-based geopolymer mortar. Constr Build Mater 2018;175:41–54.
[116] Ma C, Awang AZ, Omar W. Structural and material performance of geopolymer concrete: a review. Constr Build Mater 2018;186:90–102.
[117] Bernal SA, San Nicolas R, Myers RJ, Mejía de Gutiérrez R, Puertas F, van Deventer JSJ, et al. MgO content of slag controls phase evolution and structural changes induced by accelerated carbonation in alkali-activated binders. Cement Concr Res 2014;57(3):33–43.
[118] Talukdar S, Banthia N, Grace JR. Carbonation in concrete infrastructure in the context of global climate change—Part 1: experimental results and model development. Cem Concr Compos 2012;34(8):924–30.
[119] Zhang ZH, Provis JL, Ma X, Reid A, Wang H. Efflorescence and subflorescence induced microstructural and mechanical evolution in fly ash-based geopolymers. Cem Concr Compos 2018;92:165–77.
[120] Allahverdi A, Kani EN, Shaverdi B. Carbonation versus efflorescence in alkali-activated blast-furnace slag in relation with chemical composition of activator. Int J Civ Eng 2017;15(4):565–73.
[121] Kani EN, Allahverdi A, Provis JL. Efflorescence control in geopolymer binders based on natural pozzolan. Cem Concr Compos 2012;34(1):25–33.
[122] Provis JL, Duxson P, van Deventer JSJ, Lukey GC. The role of mathematical modelling and gel chemistry in advancing geopolymer technology. Chem Eng Res Des 2005;83(7):853–60.
[123] Škvára F, Kopecký L, Smilauer V, Bittnar Z. Material and structural characterization of alkali activated low-calcium brown coal fly ash. J Hazard Mater 2009;168(2–3):711–20.
[124] Bortnovsky O, Dědeček J, Tvarůžková Z, Sobalik Z, Šubrt J. Metal ions as probes for characterization of geopolymer materials. J Am Ceram Soc 2008;91(9):3052–7.
[125] Hamidi RM, Man Z, Azizli KA. Concentration of NaOH and the effect on the properties of fly ash based geopolymer. Proc Eng 2016;148:189–93.
[126] Zhang ZH, Provis JL, Reid A, Wang H. Fly ash-based geopolymers: the relationship between composition, pore structure and efflorescence. Cement Concr Res 2014;64(10):30–41.
[127] Martín-Pérez B, Zibara H, Hooton RD, Thomas MDA. A study of the effect of chloride binding on service life predictions. Cement Concr Res 2000;30(8):1215–23.
[128] Tuutti K. Corrosion of steel in concrete. Swedish Foundation Concr Res Stockholm 1982;20(5):105–19.
[129] Wang SD, Huang YB, Wang Z. Concrete resistance to chloride ingress: effect of cement composition. J Chin Ceram Soc 2000;28(6):570–4. Chinese.
[130] Xie YJ, Ma KL, Long GC, Shi MX. Influence of mineral admixture on chloride ion permeability of concrete. J Chin Ceram Soc 2006;34(11):1345–50. Chinese.

Please cite this article as: A. Wang, Y. Zheng, Z. Zhang et al., The Durability of Alkali-Activated Materials in Comparison with Ordinary Portland Cements and Concretes: A Review, Engineering, https://doi.org/10.1016/j.eng.2019.08.019

[131] Shi HS, Wang Q. Research on the factors influencing on the chloride ingression in concrete. J Build Mater 2004;7(3):286–90. Chinese.
[132] Li CL, Lu XY. Rapid test method for determining chloride diffusivities in cementicious materiais. Ind Constr 1998;28(6):41–3. Chinese.
[133] Yang LF, Cai R, Yu B. Formation mechanism and multi-factor model for surface chloride concentration of concrete in marine atmosphere zone. Chin Civil Eng J 2017;50(12):46–55. Chinese.
[134] Shakouri M, Trejo D. A study of the factors affecting the surface chloride maximum phenomenon in submerged concrete samples. Cem Concr Compos 2018;94:181–90.
[135] Wang JG, Zhang JX, Guo YY, Zhou TJ. Influence mechanism of different factors on chloride ion penetration of concrete. Concrete 2018;8:49–53. Chinese.
[136] Liu JL, Fang Z. New method to calculate chloride ion diffusion in concrete under influences of multiple durability factors. J Build Mater 2013;16 (5):777–81. Chinese.
[137] Li QL, Shi CJ, He FQ, Xu S, Hu X, Wang XG, et al. Factors influencing free chloride ion condensation in cement-based materials. J Chin Ceram Soc 2013;41(3):320–7. Chinese.
[138] Shi CJ, Zhang LY, Zhang J, Li N. Ou ZH. Advances in testing methods and influencing factors of chloride ion transport properties of alkali-activated materials. Mater Rev 2017;31(15):95–100. Chinese.
[139] Zhang YS, Sun W, Sha JF, Liu ZJ. Preparation and properties of fly ash based geopolymer concrete. Chin Concr Cem Prod 2003;2:13–5. Chinese.
[140] Ravikumar D, Neithalath N. Electrically induced chloride ion transport in alkali activated slag concretes and the influence of microstructure. Cement Concr Res 2013;47(5):31–42.
[141] Park JW, Ann KY, Cho CG. Resistance of alkali-activated slag concrete to chloride-induced corrosion. Adv Mater Sci Eng 2015;2015:1–7.
[142] Thomas RJ, Ariyachandra E, Lezama D, Peethamparan S. Comparison of chloride permeability methods for alkali-activated concrete. Constr Build Mater 2018;165:104–11.
[143] Gevaudan JP, Campbell KM, Kane TJ, Shoemaker RK, Srubar III WV. Mineralization dynamics of metakaolin-based alkali-activated cements. Cement Concr Res 2017;94:1–12.
[144] Ma QM, Nanukuttan SV, Basheer PAM, Bai Y, Yang CH. Chloride transport and the resulting corrosion of steel bars in alkali activated slag concretes. Mater Struct 2015;49(9):1–15.
[145] Krizan D, Zivanovic B. Effects of dosage and modulus of water glass on early hydration of alkali–slag cements. Cement Concr Res 2002;32 (8):1181–8.
[146] Bernal SA, Provis JL, Rose V, Mejía de Gutierrez R. Evolution of binder structure in sodium silicate-activated slag-metakaolin blends. Cem Concr Compos 2011;33(1):46–54.
[147] Lloyd RR, Provis JL, van Deventer JSJ. Pore solution composition and alkali diffusion in inorganic polymer cement. Cement Concr Res 2010;40 (9):1386–92.
[148] Zhu HJ, Zhang ZH, Zhu YC, Tian L. Durability of alkali-activated fly ash concrete: chloride penetration in pastes and mortars. Constr Build Mater 2014;65(13):51–9.
[149] Zhou YH. Effects of recycled aggregate on mechanical and durability properties of high calcium ash geopolymer concrete. Sci Tech Eng 2017;17 (11):295–300. Chinese.
[150] Su Y, Wang ZH, Wang YB, Wang XJ, Wei XC, Zeng SH, et al. Strength and resistance to chloride ion penetration of fiber reinforced alkali-activated slag concrete. J Hubei Univ Tech 2017;32(1):19–21. Chinese.
[151] Shi JJ, Deng CH, Zhang YM. Early corrosion behavior of rebars embedded in the alkali-activated slag mortar. J Build Mater 2016;19(6):969–75.
[152] Chen Q, Chong G, Yang CH. Effect of mineral admixture on chloride ion permeability of alkali slag concrete. Chin Con Cem Prod 2008;3:11–3. Chinese.
[153] Zhang LF, Chen JX, Li SW. Examination study of alkali-activated slag-lithium slag concrete. J Build Mater 2006;9(4):488–92. Chinese.
[154] Khan MSH, Kayali O, Troitzsch U. Chloride binding capacity of hydrotalcite and the competition with carbonates in ground granulated blast furnace slag concrete. Mater Struct 2016;49(11):4609–19.
[155] Ke XY, Bernal SA, Provis JL. Uptake of chloride and carbonate by Mg–Al and Ca–Al layered double hydroxides in simulated pore solutions of alkali-activated slag cement. Cement Concr Res 2017;100:1–13.

Please cite this article as: A. Wang, Y. Zheng, Z. Zhang et al., The Durability of Alkali-Activated Materials in Comparison with Ordinary Portland Cements and Concretes: A Review, Engineering, https://doi.org/10.1016/j.eng.2019.08.019